

APPLICATION OF TauSpinner FOR STUDIES ON  
 $\tau$ -LEPTON POLARIZATION AND SPIN  
CORRELATIONS IN  $Z$ ,  $W$  AND  $H$  DECAYS  
AT THE LHC\* \*\*

A. KACZMARSKA<sup>a</sup>, J. PIATLICKI<sup>b</sup>, T. PRZEDZIŃSKI<sup>b</sup>  
E. RICHTER-WĄS<sup>c</sup>, Z. WĄS<sup>a,d</sup>

<sup>a</sup>The H. Niewodniczański Institute of Nuclear Physics PAN  
Radzikowskiego 152, 31-342 Kraków, Poland

<sup>b</sup>The Faculty of Physics, Astronomy and Applied Computer Science  
Jagiellonian University

Łojasiewicza 11, 30-348 Kraków, Poland

<sup>c</sup>Institute of Physics, Jagiellonian University

Łojasiewicza 11, 30-348 Kraków, Poland

<sup>d</sup>CERN PH-TH, CH-1211 Geneva 23, Switzerland

*(Received May 21, 2014; revised version received September 9, 2014)*

The  $\tau$  lepton plays an important role in the physics program at the Large Hadron Collider. Spin of the  $\tau$  lepton represents an interesting phenomenological quantity which can be used for separation of signal from background in searches for New Physics processes or in measuring properties of New Particles decaying to  $\tau$  leptons. A proper treatment of  $\tau$  spin effects in the Monte Carlo simulations is important for understanding the detector acceptance and for measurements of  $\tau$  polarization and  $\tau$  spin correlations. The TauSpinner package is a software tool allowing to modify  $\tau$  spin effects in any event sample containing  $\tau$  leptons. By calculating spin weights, attributed on the event-by-event basis, it enables numerical evaluation and/or modification of the spin effects on experimentally measured distributions. We review a selection of simple distributions which can be used to monitor longitudinal spin effects in  $\tau$  decays. New methods, with respect to previous publications, for validation of spin content of the user-prepared event sample are provided.

DOI:10.5506/APhysPolB.45.1921

PACS numbers: 14.60.Fg, 13.35.Dx, 02.70.Uu

---

\* Funded by SCOAP<sup>3</sup> under Creative Commons License, CC-BY 3.0.

\*\* This project is financed in part from funds of the Polish National Science Centre under decisions DEC-2011/03/B/ST2/00107 (T.P.,J.P.), DEC-2011/03/B/ST2/02632 (Z.W.), DEC-2011/03/B/ST2/00220 (E.R.W.) and 2012/07/B/ST2/03680 (A.K.).

## 1. Introduction

The research programme of LHC experiments involves careful analysis of various final states. A multitude of interesting observables have been proposed over the years [1–3]. One of the useful physics quantities is the spin state of the final state  $\tau$  leptons. For the processes like the charged or neutral Higgs boson production and their respective important backgrounds from single  $W$  or single  $Z$  production, the spin effects can be measured [4, 5] and used for optimizing signal from background separation. Spin of the final state  $\tau$  lepton carries information about the process in which  $\tau$  has been produced and manifests itself in kinematical distributions of the  $\tau$  decay products. A multitude of  $\tau$  decay channels are experimentally accessible. The dominant ones are  $\tau^\pm \rightarrow l^\pm \nu_l \nu_\tau$ ,  $\tau^\pm \rightarrow \pi^\pm \nu_\tau$  and  $\tau^\pm \rightarrow \rho^\pm \nu_\tau \rightarrow \pi^\pm \pi^0 \nu_\tau$ . The decay channels listed above represent more than 70% of the total  $\tau$  lepton decay width. In all these channels, spin effects affect the energy spectra of the visible  $\tau$  decay products, but for each channel differently. Spin measurements can also be performed in the  $\tau^\pm \rightarrow a_1^\pm \nu_\tau$  channel [6, 7], however more sophisticated distributions are necessary and thus they will not be discussed here.

The paper concentrates on describing strategy for validating  $\tau$  spin effects<sup>1</sup> in the analyses at the LHC, which can be performed with help of the `TauSpinner` [8, 9] program. For that purpose, we recall simple distributions used for evaluation of  $\tau$  spin effects at LEP [7, 10, 11] — the fractions of  $\tau$  lepton energy carried by its visible decay products. We also provide methods to verify if for the particular sample the spin effects can be observed. These distributions can be used as a validation check if spin effects were properly generated and provide important input for feasibility studies of experimental analysis.

The `TauSpinner` package can be used to modify  $\tau$  spin effects in any event sample containing  $\tau$  leptons. Thus, it appears particularly useful in case events have been already generated and processed with CPU-intensive simulation of the detector response. There is no need to recreate the sample with different spin effects, as they can be altered by weights calculated by the `TauSpinner`. The solution may be very helpful to estimate the sensitivity of the sample to its spin content as one can use fully correlated samples, hence reducing the effects from statistical fluctuations. Finally, with this strategy, at very low CPU-cost generation of spin effects can be validated.

The paper is organized as follows. In Sec. 2 we recall main properties of the `TauSpinner` algorithm and in Sec. 3 explain details on the event samples

---

<sup>1</sup> The transverse  $\tau$  spin effects are not yet implemented in `TauSpinner`. These, however, become relevant only if directions of  $\pi^0$  and  $\pi^\pm$  can be experimentally distinguished. The implementation needs the complete spin density matrix of the produced  $\tau$  pair to be provided.

used for providing numerical results. In Sec. 4, we describe the properties of  $\tau$  lepton spin effects which may be of interest at the LHC and how they are transmitted to  $\tau$  decay products. In subsections, we discuss the semi-analytical formulae for spectra of leptons and single  $\pi$ s from  $\tau$  decays and the impact of QED bremsstrahlung on these spectra, which can be also described in semi-analytical form. In the following subsections we describe plots we propose for benchmarking spin effects and provide examples and short discussion on numerical results. In Sec. 5, we describe technical details about installation of the example programs. The summary, Sec. 6, closes the paper. The complete set of automatically generated benchmarking plots is collected in Appendices of a preprint version of our paper. This documents the output from new, more advanced set of example programs for using TauSpinner libraries.

## 2. TauSpinner brief description

The TauSpinner is a program associated with Tauola++ [12], enabling calculation of weights for the previously generated or constructed by other means events. For example, it is applicable to embedding technique, where  $Z \rightarrow \mu^+ \mu^-$  events are selected from data and muons are replaced by the  $\tau$  leptons with simulated decays [13]. The events must feature kinematics of  $\tau$ -lepton production and decay products, but event-by-event information on partons from which intermediate resonance decaying to  $\tau$ s was produced is assumed to be unknown, and therefore is not used. From this information alone, for each event, the algorithm calculates a spin weight corresponding to a presumed configuration, for example Higgs or  $Z/\gamma^*$  production and decay. The part of the weight related to the production of  $\tau$ -lepton pair (or  $\tau$  lepton and associated with its production  $\nu_\tau$  in the case of *e.g.*  $W$  mediated processes) is calculated only from the four-momenta of the  $\tau$ - $\tau$  ( $\tau$ - $\nu_\tau$ )-lepton pair. The information on flavours of the initial state partons, quarks or gluons, are attributed stochastically on the basis of matrix elements for parton level hard processes and parton density functions (PDFs) of the choice. By default, processes mediated by a single  $W$ ,  $Z/\gamma^*$  production are assumed. Alternative processes, like Higgs-mediated processes, can be used as well, but the intermediate state has to be present in the event record. For each  $\tau$  lepton, the decay part of the weight is calculated from the matrix element of the corresponding  $\tau$  decay channel, as classified by the algorithm. For this purpose, the matrix elements of Tauola++ library are used. In order to calculate the weight, the four-momenta of  $\tau$ -decay products need to be boosted into the  $\tau$  rest-frame. This requires careful treatment of possible rounding errors.

The weight constructed with help of the `TauSpinner`,  $WT$ , is factorized into multiplicative components: production ( $wt_{\sigma_{\text{prod}}}$ ), decay ( $wt_{\Gamma_{\text{decay}}^{\pm}}$ ) and spin correlation/polarization ( $wt_{\text{spin}}$ ):

$$\begin{aligned} WT &= wt_{\sigma_{\text{prod}}} wt_{\Gamma_{\text{decay}}^{\tau^+}} wt_{\Gamma_{\text{decay}}^{\tau^-}} wt_{\text{spin}}, \\ wt_{\text{spin}} &= R_{i,j} h_{\tau^+}^i h_{\tau^-}^j. \end{aligned} \quad (1)$$

In the present document, we focus on the last component of the weight  $WT$ , the spin weight  $wt_{\text{spin}}$ . Discussion of the other ones ( $wt_{\sigma_{\text{prod}}}$ ,  $wt_{\Gamma_{\text{decay}}^{\tau^+}}$  and  $wt_{\Gamma_{\text{decay}}^{\tau^-}}$ ) can be found elsewhere [9]. The definition of the spin correlation matrix  $R_{i,j}$  and polarimetric vectors for the decay of  $\tau$  leptons  $h_{\tau^+}^i$ ,  $h_{\tau^-}^j$  is rather lengthy and documented in our previous publications [10, 14, 15]. For the sake of the present discussion, it is important to recall only that  $h_{\tau^+}^i$ ,  $h_{\tau^-}^j$  are defined completely from the kinematics of the corresponding  $\tau$ -decay products and  $R_{i,j}$  from the  $\tau$ -production kinematics.  $wt_{\text{spin}}$  satisfies  $0 < wt_{\text{spin}} < 4$  by construction. The average of  $wt_{\text{spin}}$  on inclusive event sample equals to unity up to statistical error.

With the  $wt_{\text{spin}}$  weight one can evaluate on event-by-event basis spin effects transmitted from the production to the decay of  $\tau$  leptons. By definition,  $wt_{\text{spin}} = 1$  if those effects are ignored. Consequently, reweighting each event by  $WT = 1/wt_{\text{spin}}$  removes spin effects from the generated sample.

Also, the cases when only a part of spin effects is taken into account, more specifically the spin correlation but not the effects due to vector and axial couplings to the intermediate  $Z/\gamma^*$  state<sup>2</sup>, can be treated with the help of the appropriate weights.

### 3. Analysed event samples

We use samples of events from  $pp$  collision at 8 TeV center-of-mass energies, featuring final states of  $\tau$ -lepton pairs with a mass close to that of the  $Z$  or  $W$ , generated with `Pythia8165` Monte Carlo [16], each of 10M events. For the generation of multiphoton final state radiation in  $Z$  and  $W$  decays, `Photos++ v3.54` Monte Carlo [17] was used. The default<sup>3</sup> initialization parameters of `Pythia`, are used and no selection criteria are applied

<sup>2</sup> To  $\tau$  leptons or to incoming quarks only.

<sup>3</sup> `PartonLevel:FSR=off; WeakDoubleBoson:ffbar2WW=on; 24:onMode=off; 24:onIfAny=15; 24:mMax=125; WeakSingleBoson:ffbar2gmZ=on; 23:onMode=off; 23:onIfAny=15; 23:mMin=88; 23:mMax=94; pythia.init(2212, 2212, 8000.0); Tauola::setRadiation(false); Photos::setExponentiation(true); Photos::suppressAll(true); Photos::forceBremForDecay(2,23,15,-15); Photos::forceBremForDecay(2,-24,15,-16); Photos::forceBremForDecay(2,24,-15,16); Photos::createHistoryEntries(true,3);`

on the kinematics of outgoing  $\tau$ s. The decays of  $\tau$  leptons are generated with `Tauola++ v1.1.4` initialized with standard options<sup>4</sup>. The samples were generated including spin effects (polarization and correlations): we will refer to these samples as *polarized* samples. Starting from the *polarized* samples, depending on the studied effects, the spin effects are removed, with the help of `TauSpinner` weights. This way the *unpolarized* samples were obtained.

Additionally, we have created sample of events originating from the spin-0 resonance of the mass of  $Z$  boson and couplings of the Higgs boson, denoted as  $\Phi$  resonance. For convenience, this was performed using  $Z \rightarrow \tau\tau$  events generated with `Pythia8` Monte Carlo and  $\tau$  leptons decaying with `Tauola++` configured for the scalar resonance decay. Such events, denoted in this paper as  $\Phi \rightarrow \tau\tau$  events, serve to illustrate spin effects between  $\tau$  pairs originating from the decay of a vector or a scalar boson of the same mass and width. Please, note that `TauSpinner` weights could as well be used to reweight complete  $Z \rightarrow \tau\tau$  events to obtain  $\Phi \rightarrow \tau\tau$  events. However, this procedure introduces large statistical fluctuations due to large span of weights when going from vector-to-scalar resonance decays.

For some auxiliary tests, discussed in Sec. 4.5, we used 1M events from Drell–Yan  $pp \rightarrow Z/\gamma^* \rightarrow \tau\tau$  process generated within the virtuality interval of  $m_{\tau\tau} = 1.0\text{--}1.5$  TeV.

#### 4. Physics motivation of test observables and numerical results

In the analysis of experimental data, it is important to evaluate effects due to particular theoretical phenomena, incorporated in tools used in preparation of the experimental distributions where, at the same time, all experimental effects are taken into account. Only then, one can decide if the studied effects are sizable and can be distinguished from effects such as *e.g.* background contamination. Distortion of the energy spectra of decay products due to polarization of  $\tau$  leptons and spin correlations are examples of such effects.

Due to the short lifetime and parity-violating decays,  $\tau$  leptons are the only leptons whose spin information is transmitted to the kinematics of the observed decay products. In the  $\tau$ -lepton decay, the neutrino(s) escapes detection, so the complete final state cannot be fully reconstructed. We assume, however, that  $\tau$ -decay channel can be correctly determined and, for the sake of definition of the test distribution, that the fraction of  $\tau$  energy carried by all observable decay products combined can be used. This leads to relatively simple semi-observables even if still does not explore all correlations and energy fractions of the secondary decay products ( $\rho, a_1 \dots$ ).

---

<sup>4</sup> In general, QED bremsstrahlung was not taken into account in  $\tau$  decays. Only for preparation of Fig. 3,  $\tau$  leptons were re-decayed with QED bremsstrahlung ON or OFF.

It would be optimal to measure energies of individual  $\tau$ -decay products and use all of them simultaneously achieving then substantial gain in the sensitivity to the spin. That is the case, for example, in  $\tau^\pm \rightarrow \rho^\pm \nu_\tau \rightarrow \nu_\tau \pi^\pm \pi^0$  decay channel. The difference between  $\pi^\pm$  and  $\pi^0$  energies is determined by the spin of  $\rho$  which, in turn, carries information on the spin of the  $\tau$ .

Such effects are taken into account in `TauSpinner` algorithms but are not explored with the distributions we study in this paper. Let us remind that precision tests of the Standard Model were performed at LEP 1, with significant and well documented effort on experimental, theoretical and computational levels [18, 19]. In particular, manifestation of  $\tau$ -lepton polarization in its all main decay channels was carefully explored [7] in the context of measuring the intermediate  $Z$  boson properties. In our discussion, we recall some of the phenomenological and technical considerations of that time [10, 11], which may be useful for the LHC applications, as shown in Ref. [14]. In the LEP 1 analyses, observables were at first limited to the fraction of  $\tau$  energy carried by its observable decay products,  $x$ . Such fractions could have been used directly at LEP 1 experiments because  $\tau$  energy was equal to the beam energy. In general, in  $m_\tau \ll M_{Z,W}$  limit, the fraction  $x$  is independent from the boost and remain the same in the rest frame of intermediate  $Z$  (or  $W$ ) or in the laboratory frame. That is why it is of potential interest as a first step in preparation of the spin measurements at the LHC experiments, or to validate the correctness of spin implementation in the generated samples, even though  $x$  is not reconstructed experimentally. Because of the simplicity and direct relation to properties of the decay matrix elements, the  $x$  variable is also a good choice for Monte Carlo benchmarks<sup>5</sup> on polarization and spin correlation effects.

#### 4.1. Semi-analytical formulae

The pattern of the  $\tau$  response to spin can be studied by the Monte Carlo methods through its decay, taking into account the complexity of multi-dimensional signatures. We return to this issue later in the paper. Nonetheless in some cases, simple analytical formulae are available and can be quite helpful to visualize the effects in an intuitive way.

In the case of  $\tau^\pm \rightarrow \pi^\pm \nu_\tau$  and  $\tau^\pm \rightarrow l^\pm \nu_l \nu_\tau$  decays, formulae for energy spectra for visible decay products, neglecting mass and QED bremsstrahlung effects, have been known for a long time [10]. For  $\tau^\pm \rightarrow \pi^\pm \nu_\tau$ , it is

$$1 + P \times (2x - 1) \tag{2}$$

---

<sup>5</sup> Our definitions follow Refs. [10, 11, 14]. At LEP 1 time, the  $x$  fraction was the actual observable; for the collisions of the center-of-mass energy close to the  $Z$  peak, the  $\tau$ -lepton energies were close to the beam energies. The  $x$  variable received a lot of phenomenological attention.

and for  $\tau^\pm \rightarrow \ell^\pm \nu_\ell \nu_\tau$  ( $\ell = e, \mu$ ), it reads

$$\frac{5}{3} - 3x^2 + \frac{4}{3}x^3 - P \times \left( -\frac{1}{3} + 3x^2 - \frac{8}{3}x^3 \right), \quad (3)$$

where  $P$  denotes  $\tau$  polarization and  $x$  is a fraction of  $\tau^\pm$  energy carried by  $\pi^\pm$  or  $\ell^\pm$ .

These analytic forms of the spectra can be extended to the case when effects of radiative corrections are taken into account, see *e.g.* formulae<sup>6</sup> A3 and A4 of Ref. [11]. In that case, the parametrization of the spectra depends on experimental treatment of photons in vicinity of  $e$ ,  $\mu$  or  $\pi^\pm$  ( $\pi^0$ ).

For tests presented here, we assume that bremsstrahlung in decays is not taken into account in the event generation or that its effect can be neglected. Also, that the mass terms (non-negligible for muons) can be neglected. Otherwise, the semi-analytical formulae would become much more complicated. With time, as it was the case of LEP [7], these effects may become of interest as well. It is straightforward to introduce effects due to bremsstrahlung to formulae (2), (3); not only in  $\tau$  decay itself, but also in decay of intermediate  $Z$  or  $W$  bosons.

With above assumptions, simple formulae (2), (3) can be fitted to histograms of energy fractions  $x$ , to evaluate effective polarization  $P$  and conclude if the particular sample features the spin effect and/or if this effect is big enough to be statistically significant.

In case a semi-analytical formula is not available for the distribution, or distribution is distorted by kinematical selection, one can use for fitting the linear combination of reference spectra corresponding to pure left-handed and right-handed  $\tau$  leptons. This template fit technique was already used by LEP experiments [7]. Such reference spectra can be obtained with the help of Monte Carlo methods.

#### 4.2. Spin correlations and polarization monitoring plots

It is expected that in most cases of interest at the LHC,  $\tau$  leptons are produced through the decay of intermediate states of  $W$ ,  $Z/\gamma^*$  or  $H$  bosons. Because of the detector properties, fraction of  $\tau^\pm$  energy carried by visible decay products, respectively  $x_1$  ( $\tau^+$ ) and  $x_2$  ( $\tau^-$ ), is a natural choice for the monitoring variables. Those variables are not directly measurable at the LHC and thus of a limited use for the experimental analyses, however they were partly adapted to the LHC applications already in [14].

The example spectra of  $x_{1,2}$  for the specific  $\tau$ -decay channels are shown in Fig. 1 for  $Z \rightarrow \tau^+ \tau^-$  decays, separately for leptonic (Fig. 1 (a)), single  $\pi$  (Fig. 1 (b)) and  $2\pi$  decay channels (Fig. 1 (c)). For construction of these plots, the *polarized* event sample, discussed in Sec. 3, was used.

<sup>6</sup> Unfortunately, this review is known to have typing mistakes.

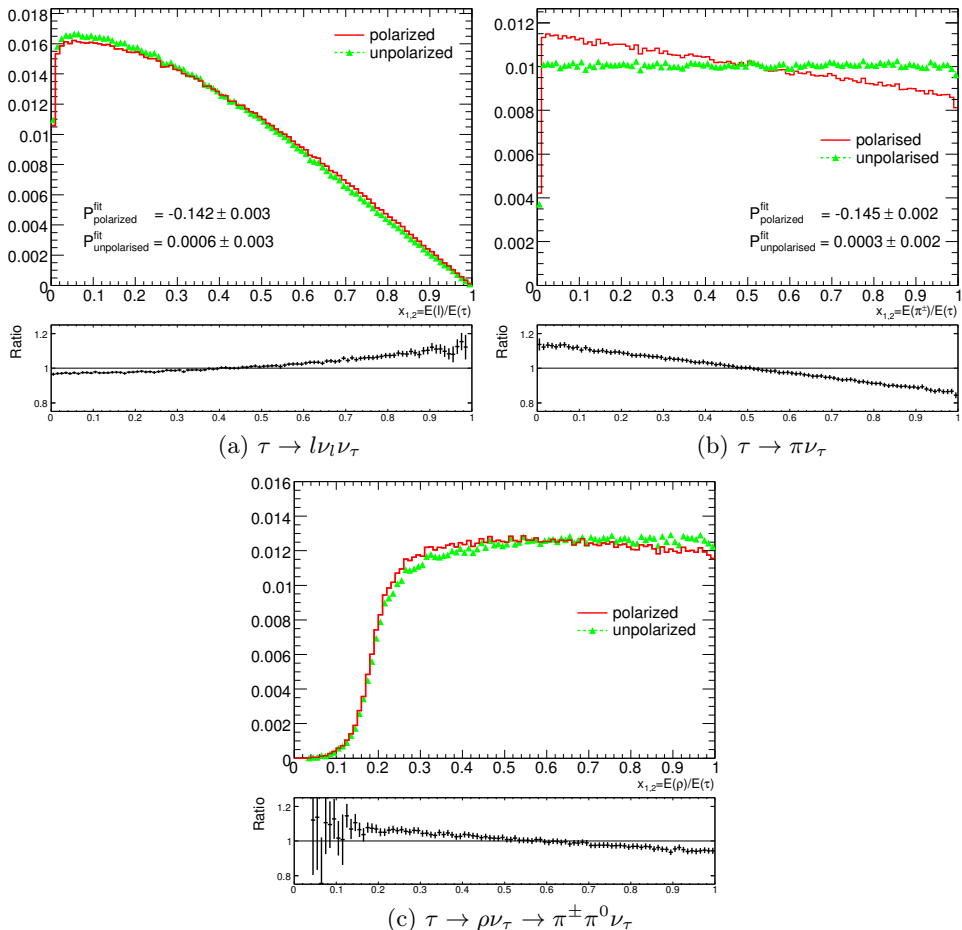


Fig. 1. The spectra of visible  $\tau$  decay energy normalized to  $\tau$  energy,  $x_{1,2}$ . Spin effects included (solid line/red) and neglected (dashed line with triangles/green). The  $\tau$  leptons are produced through  $Z$  decay close to the mass peak. The  $\tau$  polarization  $P$  is obtained from the fit to the distributions constructed from  $Z \rightarrow \tau\tau$  sample for polarized and unpolarized cases. For the fit, the first bin in the  $\tau \rightarrow \pi\nu$  case and first five bins in the  $\tau \rightarrow l\nu_l\nu_\tau$  case where mass effects would be the largest, were omitted.

The unpolarized spectra were obtained from the *polarized* sample, using weights calculated by TauSpinner. From the comparison of the two spectra, the effect of polarization can be evaluated. As shown in Fig. 1, the spectra and their sensitivity to the spin vary dramatically depending on the  $\tau$ -decay channel. Negative polarization leads to harder spectra in the case of  $\tau \rightarrow l\nu_l\nu_\tau$  decays, and softer in the case of  $\tau \rightarrow \pi\nu_\tau$ . The effect is of 20% at the very end of the spectra.

Figure 1 gives also results from the fits to respectively formulae (2) and (3):  $P_{\text{polarized}} = -0.142 \pm 0.003$  ( $P_{\text{unpolarized}} = 0.0006 \pm 0.003$ ) for leptonic mode and  $P_{\text{polarized}} = -0.145 \pm 0.002$  ( $P_{\text{unpolarized}} = 0.0003 \pm 0.002$ ) for single  $\pi$ -decay mode. Note that the differences between the results for the leptonic and  $\pi$  modes, even though formula (3) is missing mass corrections for muons, are small. This is because the first bins of the histograms were excluded from fitting. The nominal average  $\tau$  polarization of sample used, as estimated by the TauSpinner, reads  $P = -0.144 \pm 0.001$ . The missing muon mass alters by less than  $-0.005$  the polarization obtained from the fit

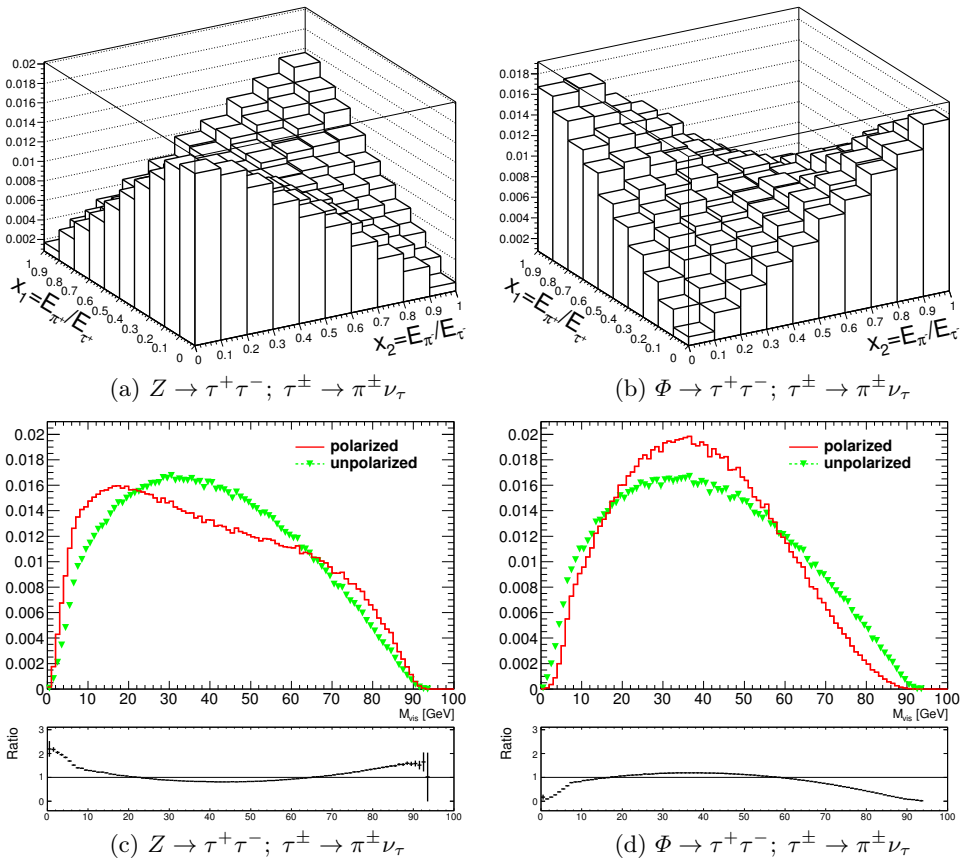


Fig. 2. The case of  $Z(\Phi) \rightarrow \tau^+ \tau^-; \tau^\pm \rightarrow \pi^\pm \nu_\tau$ . On plots (a), (b): lego plots of  $E_{\pi^+}/E_{\tau^+} \times E_{\pi^-}/E_{\tau^-}$  and on (c), (d): invariant mass distributions of visible  $\tau^+$  and  $\tau^-$  decay products are shown. In the case when spin effects are included solid line/red, otherwise dashed line with triangles/green is used. For plots (a), (c): the  $\tau$  leptons produced through  $Z$  decay are used. For plots (b), (d):  $\tau^+ \tau^-$  pairs from spin-0 state  $\Phi$  are used. All distributions are normalized to unity.

to distribution in the leptonic channel, both for the polarized and unpolarized samples. Statistical errors on the fit results correspond to samples of 10M events, as discussed in Sec. 3. Although fit results are not precise (they are biased by approximations of analytic formulae (2), (3)), some distinguishing power between polarized and unpolarized sample is demonstrated. Statistical errors on the fitted values are calculated by the RooFit fitting package [20].

The spin correlation manifests itself differently depending on the particular  $\tau^+$ - and  $\tau^-$ -decay channels. In Fig. 2 (a) and Fig. 2 (b), we provide the two-dimensional plots (lego plots) of  $E_{\pi^+}/E_{\tau^+} \times E_{\pi^-}/E_{\tau^-}$  for the case of  $Z(\Phi) \rightarrow \tau^+\tau^-; \tau^\pm \rightarrow \pi^\pm\nu_\tau$  and the distributions of invariant mass  $M_{\text{vis}}$  for the all visible  $\tau$ -pairs decay products combined, Fig. 2 (c) and Fig. 2 (d). Note that to a good approximation  $M_{\text{vis}} = Qx_1x_2$ , where  $Q$  denotes mass of the  $\tau$  pair. In the case of spin-0 state  $\Phi$ , the fast-fast ( $x_{1,2} > 0.5$ ) and slow-slow ( $x_{1,2} < 0.5$ ) pairs of  $\pi^\pm$  are disfavoured, whereas in the  $Z/\gamma^*$  case the fast-slow and slow-fast combinations are less populous. Each configuration of  $\tau$ -decay channels feature different spin response pattern. We refer the reader to series of plots in Appendices (attached to the preprint version of our paper) collecting automatically created numerical results for  $W$ ,  $Z/\gamma^*$  and  $\Phi$  cases, and different configurations of the  $\tau$ -decay modes. The short summary is given in Sec. 4.6. The Appendices represent examples of output from programs described in Sec. 5.

#### 4.3. Fits to energy fractions, radiative corrections and experimental cuts

Deformation of the spectra due to radiative corrections are presented in Fig. 3. As explained in Ref. [11], they can be as big as the effect of  $\tau$  polarization itself (Fig. 3 (a)). Our fit results given in the caption of Fig. 3 support this observation. Depending on whether for calculation of  $x_{1,2}$  bremsstrahlung photons are combined with the lepton or not, effect on  $\tau$  polarization obtained from the fit of formulae (3) may substantially differ in size<sup>7</sup>. The main deformations are for  $x_{1,2}$  close to 0 or 1. In general, when distributions are not sufficiently well described by formulae (2) and (3), template methods based on Monte Carlo, can be used similarly to measurements of the  $Z$  couplings performed at LEP [7].

---

<sup>7</sup> It is important to verify if such spectra with radiative corrections will be useful. Other effects, such as experimental cuts, may change shapes as well, making such theoretical improvements of a minimal interest only.

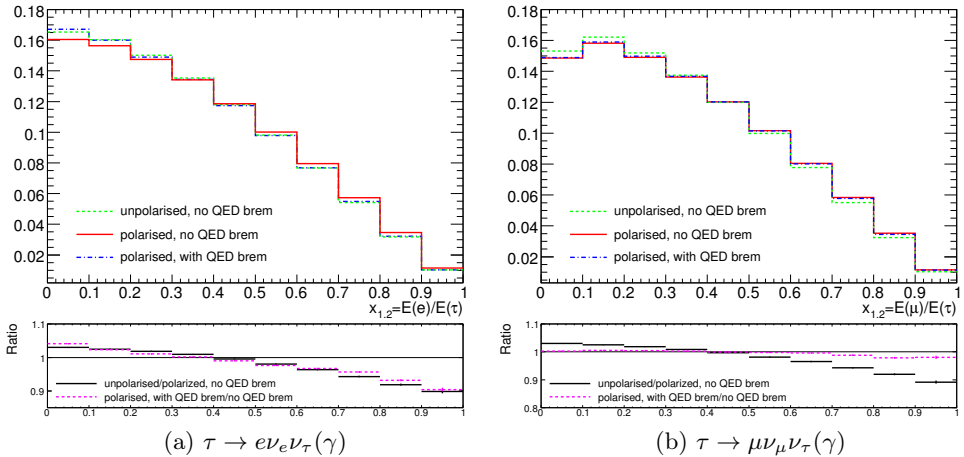


Fig. 3. Example plots for the effects of QED bremsstrahlung in leptonic decays of  $\tau$ . Spectra of visible  $\tau$ -decay energy normalized to  $\tau$  energy,  $x_{1,2}$ , are shown. Spin effects and QED bremsstrahlung are excluded for dashed line/green, for spin effects included but QED bremsstrahlung excluded solid line/red and, finally, both spin effects and QED bremsstrahlung included dotted line/blue. Distributions constructed for  $Z \rightarrow \tau\tau$  decays. Left-hand plot is for  $\tau$  decays to electron, right-hand plot for  $\tau$  decays to muons. For the plots, histograms were rebinned. For the fits of histograms, all 100 bins except the first five (that is exactly as in fits for Fig. 1) were used. The expression (3) was fitted to the spectra. For the  $e$  channel,  $P = 0.004 \pm 0.002, -0.141 \pm 0.002, -0.015 \pm 0.002$  respectively for unpolarized, polarized and polarized with bremsstrahlung effect included cases. For the  $\mu$  channel, the analogous result reads  $P = -0.009 \pm 0.002, -0.153 \pm 0.002, -0.124 \pm 0.002$ . The ratios of plots: no QED bremsstrahlung, polarized/unpolarized and polarized, no QED bremsstrahlung/with QED bremsstrahlung are also presented.

#### 4.4. From benchmarks toward realistic experimental distributions.

Numerical results presented above were prepared in an idealized case, where no experimental selection was applied to the analysed samples. We have relied on the unobservable fractions of visible  $\tau^\pm$  energies,  $x_1$  and  $x_2$ . This is well suited for testing Monte Carlo programs and detector simulation. In Fig. 4, we show the impact of spin effects on experimentally observable and sensitive to spin quantity  $E_{\pi^-}/E_{\text{vis}}$  for  $\tau^- \rightarrow \pi^- \pi^0 \pi^0 \nu_\tau$  decay channel. As one can conclude, effects of the spin are sizable. The effect can be evaluated using the TauSpinner unweighting algorithm. The  $a_1$  decay channel is less suitable for testing the programs or simulations because of more complex interpretation of different spectra. For applications in experimental data analysis, one should address possible complications like background

contamination or limited acceptance. The template fit technique [7], convenient at the LHC, as demonstrated in [4], can be used for spin in this case as well.

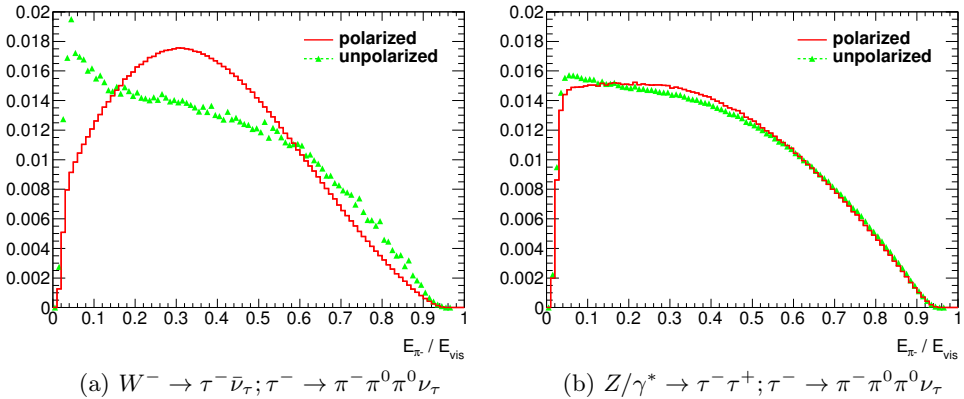


Fig. 4. Example plots for effects of spin in  $\tau^- \rightarrow \pi^- \pi^0 \pi^0 \nu_\tau$ ; the  $E_{\pi^-}/E_{\text{vis}}$  distribution. The case when spin effects are included is denoted by solid line/red, for spin effects excluded, dashed line with triangles/green is used. Left-hand side plot is for  $W^- \rightarrow \tau^- \bar{\nu}_\tau$  production, right-hand side plot for  $Z/\gamma^* \rightarrow \tau^- \tau^+$ . Note large statistical fluctuations for unpolarized distributions in the  $W$  case obtained with unweighting procedure. It is because in the case of 100% polarization like for  $W \rightarrow \tau \nu_\tau$  decays, the spin weight  $wt_{\text{spin}}$  can approach zero. Its inverse used for unweighting polarization, can therefore become arbitrarily large, resulting in (integrable) singularity of the distribution. These large fluctuations indicate the limitation for use of weights method to remove spin effects from already generated events.

#### 4.5. Consistency checks

Theoretical systematic error is of a great importance for the TauSpinner algorithm. We do not plan to review this aspect of the program development now. Some results are already documented in [8, 9], but more detailed studies will be needed when the precision requirements will become more stringent. The work with explicit multi-leg QCD matrix elements of appropriate form, like in Ref. [21], will become mandatory.

It has been known for a long time [22, 23], that predictions for the Drell–Yan processes must lead to the dependency on the polar and azimuthal angles of outgoing leptons in the center-of-mass frame of decaying resonance in the form of second order spherical harmonics. This feature leads to the broad spectrum of possible applications, from validating implementations of higher order QCD corrections in the Monte Carlo programs, to the indirect measurement of the mass of the  $W$  boson [24].

It is important to notice that in the process of preparing spin weights, TauSpinner calculates all ingredients of the effective Born parton level cross section, as described in [10, 11, 14, 15]. Predictions for other observables or quantities of phenomenological interest, such as quark level forward–backward asymmetry or probability of a given quark flavour to originate a particular hard process event, can be obtained when executing the code. Because of mentioned above properties of QCD, formulae for polarization and other quantities, remain essentially as at LEP.

If the studied sample is generated by a Monte Carlo program and *physics history entries* (flavours and momenta of quarks entering hard process) are stored, one can directly use this information to retrieve properties of the electroweak matrix elements and hadronic interactions of the studied event sample. The four-momenta and flavours of the incoming quarks can be used to calculate parton level forward–backward asymmetry or rate of production from distinct quark flavour. These results can then be compared with the similar quantities estimated from the weights calculated by the TauSpinner algorithms using kinematics of the  $\tau$  decay products only, providing test on the precision of TauSpinner algorithms.

Unfortunately, information on four momenta and flavours of incoming quarks is usually available only for Monte Carlo with parton showers based on the leading logarithm approach. At the next-to-leading logarithm level [25] such information may be available as well, but it is not necessarily the case. Because of the spin-1 nature of objects decaying to pair of leptons, the angular distributions of  $\tau$  leptons in the rest frame of  $\tau$  pair are described by spherical harmonics, of at most the order of two. This explains why higher order QCD corrections, contributing higher than second order spherical harmonics, must be small [22].

We have prepared following tests, supplementary to the ones of Subsec. 4.2, which exploit *physics history entries*. These tests may be particularly interesting if some kind of inconsistency is found in the analysed sample and one is debugging its origin:

- A. **Test of kinematic reconstruction.** In TauSpinner, to evaluate  $\tau$  scattering angle  $\theta^*$ , the algorithm described in [26] is used. Resulting  $\cos\theta^*$  is compared with  $\cos\theta$  of scattering angle calculated from *physics history entry* of the event record. The difference of the two results is monitored.
- B. **Test of electroweak Born cross section.** For the sample featuring *physics history entries*, the scattering angle of the outgoing lepton in the hard process can be calculated and appropriate angular distribution plotted separately for each flavour of incoming quarks. This distribution, in the leading log approximation has the functional form

of  $(1 + \cos^2 \theta + A \cos \theta)$ . Coefficient in front of  $\cos \theta$ , defining size of forward–backward asymmetry  $A_{\text{FB}}$ , can be obtained from the fit of this function to  $\cos \theta$  distribution obtained from the analysed sample. The same coefficient can be calculated with the help of `TauSpinner` algorithm. This calculation uses as an input information of parton density functions (PDFs) which is convoluted with the parton level matrix-element of the hard process. The average value of the coefficient  $A$  (defining size of the forward–backward asymmetry  $A_{\text{FB}}$ ) can be therefore obtained independently from the algorithm responsible for calculating spin weights and, in particular, scattering angles. The comparison of the results obtained from the fit to  $\cos \theta$  distribution constructed from *physics history entries* of the events on the one side, and of `TauSpinner` internal calculation of  $A$  (when only PDFs and virtuality of  $\tau$  pair is used) on the other side, provides tests for effective Born parameters consistency in the analysed sample and `TauSpinner` code. Results of this test depend also on the choice of PDFs and on the correctness of the `TauSpinner` algorithm for reconstruction of PDFs arguments (fractions of proton momenta carried by partons) from the kinematics of the  $\tau\tau$  (used is virtuality and pseudorapidity of the  $\tau\tau$  system).

An example of such comparison is given in Fig. 5 for the case of Drell–Yan events with virtuality in the range of 1–1.5 TeV. The fit gives  $A = 1.617 \pm 0.002$  for up quarks and  $A = 1.692 \pm 0.003$  for down quarks. From the `TauSpinner` calculation using Born amplitude, value of the  $A$  parameter averaged over the same sample (calculated from Born cross section) read 1.613 and 1.691 respectively with negligible statistical error<sup>8</sup>. For other choices of virtualities, agreement was found to be of a similar quality.

- C. **Test of PDFs.** To some level, previous test can be complemented with the direct test of PDFs. Fraction of sample events (production rates) with hard process of particular incoming quark flavour can be compared with that fraction attributed by the `TauSpinner` algorithm. In the second case, every event contribute, but with the weight proportional to quark level total cross sections multiplied by respective PDFs. For the example shown in Fig. 5, we obtained respectively: rate of down quarks 0.217 (`TauSpinner` 0.216) and rate of up quarks 0.766 (`TauSpinner` 0.762).

---

<sup>8</sup> In this case, we concentrate on matching the electroweak parameters in initialization of `Pythia` and `TauSpinner`, hence the initial state hadronic effects were switched off. We have checked that if more complete treatment is used, quality of the agreement between  $A$  and  $A^{\text{fit}}$  is degraded by  $\sim 0.01$ , but shapes of the distributions become more complicated.

The results for tests B and C depend on the PDF's used internally by TauSpinner and on effective Born-level cross section used at parton quark level. In the case of B, the dominant contribution comes from the odd power of axial couplings, whereas in the case of C even powers of the axial couplings dominate the result. That is why the two tests are to a large extent independent.

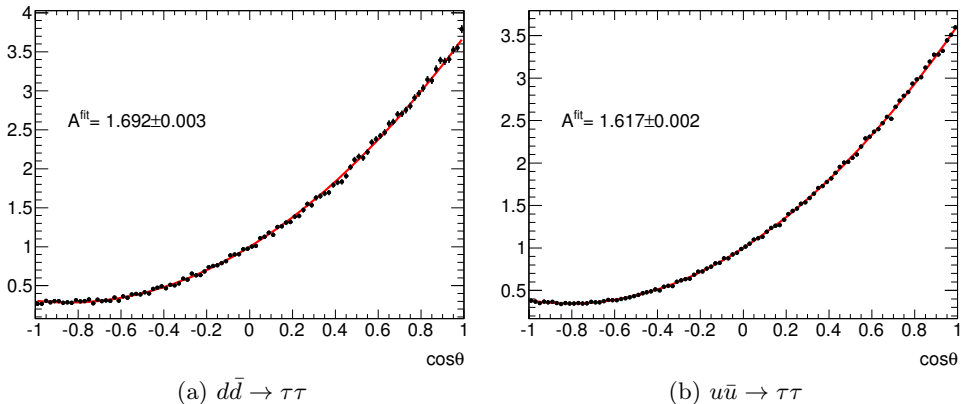


Fig. 5. Differential distribution in the hard scattering angle  $\cos\theta$  calculated from *physics history entries* in the event record, the superimposed fit of  $(1 + \cos^2\theta + A \cos\theta)$  solid line/red is shown. Histograms are normalized to  $\frac{8}{3}$  (the integral of fit function in range  $[-1, 1]$ ). The virtuality of the  $\tau\tau$  pair was restricted to the range of 1–1.5 TeV.

**D. Partial polarization test.** An option that the event sample features spin correlation of the two  $\tau$  leptons, but not fully the polarization effects due to production of intermediate state  $Z/\gamma^*$  couplings is of practical interest when constructing the so-called  $\tau$  embedded sample [13]. In that case in  $Z \rightarrow \mu\mu$  events selected from data, the muon tracks and associated energy depositions in the calorimeters are replaced by the corresponding signatures of the final state particles of the  $\tau$  decay. In this approach, essential features such as the modelling of the kinematics of the produced boson, the modelling of the hadronic activity of the event as well as contributions from pile-up are taken from data. Thereby the dependence on Monte Carlo simulation is minimized. While reintroducing only the spin correlations, it is sufficient to use information on the four-momenta of  $\tau$  leptons and their decay products thus the embedded samples have  $\tau$  spin correlation effects included. Reintroducing effects from polarization requires information on structure functions of partons forming decaying resonance, which is not available in the embedded samples. Therefore by

default,  $\tau$  polarization is not taken into account in the  $\tau$  decays in the embedded samples and the average polarization is 0. The neglected effects can be evaluated and be introduced with the help of `TauSpinner` weights, see Sec. 5.4. This, however, means introducing theoretical uncertainty due to the electroweak effective Born and of incoming quark PDFs to the sample, which *a priori*, was free from such uncertainties. If only angular dependence of the polarization is neglected, the systematic error due to PDFs on the spin effects is reduced and much smaller systematic error due to the effective electroweak Born parameters remain. The theoretical systematic error for such approach can be assigned by comparing spin effects calculated from approximation which rely on four-momenta of  $\tau$  leptons and their decay products with the one exploring full hard scattering parton level amplitudes.

In the discussion of numerical results presented above, samples without any kinematical cuts were used. However, one may be interested to test how our algorithm will perform if only a particular class of events, for example of high  $p_T$  configurations only, is used. All the tests listed above can be then performed using sub-samples defined by the particular set of cuts. In such cases, the validity of the `TauSpinner` algorithms and of the parton shower algorithm used for the sample generation can be explored in more exclusive phase-space regions.

#### 4.6. Reference plots

Let us now discuss briefly the large collection of automatically created plots prepared by our testing programs<sup>9</sup>. For the preprint version of our paper, such plots are collected into rather lengthy Appendices for the  $W$ ,  $Z/\gamma^*$  and spin-0 resonance  $\Phi$ . We have grouped the figures for each  $\tau$ -decay channel (case of  $W$ ) or for each pair of  $\tau$ -decay channels (case of  $Z$ ) separately. For leptonic and single  $\pi$ -decay channels, results of the fits to spectra (2) or (3) are given. The input samples feature complete longitudinal spin effects. The `TauSpinner` weights were used to unpolarize the sample. For the case of  $\Phi \rightarrow \tau\tau$  events, the  $Z \rightarrow \tau\tau$  sample was used, but  $\tau$  decays were regenerated instead of reweighted for better numerical stability.

For each type of decaying resonance, we give specification of the sample used for the respective set of plots, reporting the number of the analysed events with the decomposition into particular (pair of)  $\tau$ -decay channels and initialization of the generator used for sample preparation. We also plot the control distribution of invariant mass of  $\tau\tau$  ( $\tau\nu_\tau$ ) system. This sanity plot

---

<sup>9</sup> These programs are included in the `TauSpinner` distribution tar-ball. See Sec. 5 for more details.

verifies if the sample consists of events at the resonance peak or if substantial contribution from low energy or very high mass tails is included in the sample as well. Spin effects are different if events are taken at above or below the  $Z$  peak.

Afterwards, comes a collection of plots to large extend following layouts of Fig. 1 and Fig. 2:

- In the case of  $W \rightarrow \tau\nu_\tau$  decay only the one-dimensional distribution of the energy fraction carried by  $\tau$  lepton is plotted, comparing the case of polarized and unpolarized samples. In the captions of the plots, similarly as in Fig. 1, the fitted value of the  $\tau$  polarization  $P$  is given as a measure of spin sensitivity of analysed samples.
- In the case of the  $Z/\gamma^*$  mediated processes and for each particular combination of  $\tau^+$ - and  $\tau^-$ -decay channel, the set of histograms are collected. The first is the two-dimensional lego plot constructed from the fractions of energies of  $\tau^+$  and  $\tau^-$  carried by their corresponding observable decay products. Analogous lego plot is also shown for the case when spin effects are removed with the help of weights calculated by **TauSpinner**. Ratio of the two distributions is given in the lego plot of the second row. It demonstrates the strength of the spin effect. On the right-hand side of this lego plot, the one-dimensional histogram for invariant mass, of all visible products of  $\tau^+$  and  $\tau^-$  combined, is given. It provides a convenient way of representing spin correlation effects in the case of smaller samples, which may be insufficient to fill the two-dimensional distributions. The last two plots show single  $\tau^+$ - and  $\tau^-$ -decay product spectra respectively (each plot containing polarized sample, sample with modifications due to **TauSpinner** weights and their ratio). Spectra are normalized to unity. In the captions of the plots, see Fig. 1, the fitted value of  $\tau$  polarization  $P$  is given as a measure of spin sensitivity of analysed samples. Note that the groups of plots for the cases when decay channels for  $\tau^+$  and  $\tau^-$  are simply interchanged, coincide up to permutation of axes, unless some cuts are introduced by the user.
- In the case of  $\Phi$ -mediated process, set of plots analogous to  $Z/\gamma^*$ -mediated processes are given.

The proposed set of benchmark plots can be extended further with the help of provided validation programs, in particular, for the cases of partial implementation of polarization and spin correlations effects. Respective systematic errors can be evaluated.

## 5. Technical details

For the purpose of this paper, a directory `TauSpinner/examples/applications`<sup>10</sup> has been added to the previous distributions of `Tauola++`. It contains several tools used to produce the plots for this paper and to obtain necessary results. It was also extended with several tests that help validate `TauSpinner`. If `Tauola++` is configured with all prerequisites needed to compile `TauSpinner` package, as well as `TauSpinner` examples<sup>11</sup>, compiling these additional programs should not require any further setup and can be done by executing `make` in `applications` directory.

### 5.1. The applications directory

In the following subsection, we will briefly describe the sub-directories for this package and their use.

#### 5.1.1. Generating plots

The main program, `applications-plots.cxx`, generates plots which are latter included in the pdf file (like of Appendix A — available in the preprint version of the paper). It uses the same algorithm as the one used in `tau-reweight-test.cxx`; part of the examples for `TauSpinner` included in `Tauola++` tar-ball starting from version of November 2012. In this example code, input file `events.dat` is processed and for each event  $WT$  weight is calculated. The set of histograms is filled with weighted (to remove spin effects) and not weighted events, separately for each  $\tau$ -decay mode or  $\tau$ -pair decay mode combination. Histograming and plotting is done using the `ROOT` library [20] (fits are performed with the help of the `RooFit` library).

This program can be used to recreate plots from the Appendices. For this, a datafile with  $W$  and  $Z$  which decay into  $\tau$ s is needed. Note that since the template `LaTeX` file is prepared for both  $W$  and  $Z$  samples, this program can be executed on a single sample file containing both types of events or

---

<sup>10</sup> In `Tauola++ v1.1.4`, released on 12 Dec 2013, this directory was called `TauSpinner/examples/tauspinner-validation`. All subsequent directories and programs have been renamed following the new convention. In particular, directories: `applications-plots-and-paper`, `applications-rootfiles`, `applications-fits` was respectively called `tauspinner-validation-results`, `tauspinner-validation-plots`, `tauspinner-validation-fit` and programs `applications-plots.cxx`, `applications-comparison.cxx`, `applications-fits.cxx` were called `tauspinner-validation-plots.cxx`, `tauspinner-validation-comparison.cxx`, `tauspinner-validation-fit.cxx`. While the naming of programs and subdirectories changed, the content of the programs remained the same.

<sup>11</sup> Up-to-date instructions can be found on the `Tauola++` website in the documentation to the most recent version of the package [27].

on two samples with separate  $W$  and  $Z$  events<sup>12</sup>. Only channels  $\tau \rightarrow \mu\nu_\mu\nu$ ,  $\tau \rightarrow e\nu_e\nu$ ,  $\tau \rightarrow \pi\nu$  and  $\tau \rightarrow \rho\nu$  are analysed. To run the program:

- make sure that ROOT configuration is available through `root-config`,
- execute `make` in `TauSpinner/examples/applications` directory,
- verify that settings in file `applications-plots.conf` are correct, including the path to input file<sup>13</sup>,
- execute `./applications-plots.exe applications-plots.conf`.

A set of plots will be generated in the directory indicated by the configuration file (the default one is `applications-plots-and-paper`) and a breakdown of the  $\tau$ -decay channels found in the sample will be written at the end of running the program. If the input file contains both  $W$  and  $Z$  decays, two sets of plots will be generated, each accompanied with summary of the  $W$  and  $Z$  events properties. The program also saves all histograms created during processing time to `out.root` file. This file can be used to archive the results for further analysis or to add fits to the plots.

### 5.1.2. Adding fits

The code for adding fits is provided in the subdirectory `applications-fits`. It is built along with other programs when executing `make` in `applications` directory. This tool adds fits to the histograms generated by `applications-plots.exe` using the formulae (2) and (3), results of the fits are stored in the rootfile. See the `README` file in this directory for details on how input files are processed.

This program uses rootfiles from subdirectory `applications-rootfiles`. They are specified in the default configuration file `applications-fits.conf` as the input files of this program. The resulting plots, with added fit information on polarization, will be stored in `applications-plots-and-paper` directory. Previously generated plots will be overwritten. This can be changed in the configuration file with path to the output directory.

As mentioned in Sec. 4.3, the fit can be applied not to the whole range but to the interval  $(x_1, x_2)$ , that is why an option to perform fits only in the limited range of  $[x_{\min}, x_{\max}]$  has been provided in the code and is controlled by the configuration file.

---

<sup>12</sup> This program does not produce histograms stored in Appendix B (available in the preprint version of the paper). These plots require change of the PDGID of the  $Z$  boson so `TauSpinner` can calculate weight as if the intermediate boson is Higgs. This change is omitted from the example provided with the distribution tar-ball for simplicity.

<sup>13</sup> Note that example file `examples/events.dat` can be used to verify if the program compiles and runs correctly. However, it contains only a sample of 100  $Z \rightarrow \tau^+\tau^- \rightarrow \pi^+\pi^-\nu_\tau\nu_\tau$  events.

### 5.1.3. Recreating Figs. 3 and 4

The subdirectory `applications-rootfiles` contains rootfiles of histograms necessary to reproduce all plots shown in our paper. These rootfiles are used by `applications-fits.exe`. Histograms for the plots that are not part of the Appendices are also stored in the rootfiles. Executing `make` will invoke code to generate the plots for Figs. 3 and 4. Note that generation of these rootfiles requires different setup and different data samples than for any other plots. While necessary changes are straightforward, including such options would add to the already complex structure of the validation programs, thus they were skipped in the distribution.

### 5.1.4. Additional tests and tools

Two additional subdirectories:

- `test-bornAFB`
- `test-ipol`

were added for further validation of the `TauSpinner` library. These tests are somewhat peripheral to the main topic of the paper, thus they were only documented in the `README` files of the corresponding sub-directories. The result of the first test is briefly discussed in Sec. 4.5, while the second one has not been presented here. It is, however, included in the package as a validation test of `TauSpinner` options (`Ipol` = 0, 1, 2, 3).

The `applications` directory contains additional programs:

- The `hepmc-tauola-redecay.cxx`, while not being an example for `TauSpinner`, can be used to process existing input file and remove  $\tau$  decays substituting them with new ones generated by `Tauola++`. This tool can be used to generate unpolarized  $\tau$  decays needed to verify different `TauSpinner` options (see Sec. 5.4). Note, that as with `Tauola++`, generation options are limited by the available information stored in the data files.
- The `applications-comparison.cxx`, uses two input files. First one is considered as a reference. For the second one `TauSpinner` weights are used. The same set of histograms is produced for both input files and compared afterwards. This program can be used to validate `TauSpinner` options, as for example in the case of E described in Sec. 5.4.

Details of how to use both programs are described in `README` of the directory.

### 5.1.5. Generating pdf file

The subdirectory `applications-plots-and-paper` contains the LaTeX files, as well as all other files necessary to prepare Appendices of a preprint version of this paper. Executing `make` in this directory generates the pdf file as of our paper.

Text of Appendices is stored in files: `appendixA.tex` and `appendixB.tex`. The user can thus easily re-attach results of the program run to the documentation of his own project starting from the template `user-analysis.tex`; the `make user-analysis` will include Appendices into short `user-analysis.pdf`.

### 5.1.6. Final remarks

It is possible to redo, for the sake of documenting results of one own tests, all figures and other numerical results of the Appendix A (that is also of `user-analysis.pdf`). If the physics assumptions are substantially different than the one used for the present paper, shapes of the obtained distribution may differ as well. In every case, the following steps have to be followed:

1. generate a sample of  $W$  and  $Z$  decays to  $\tau$ ;  $\tau$  decaying to  $\mu, e, \pi$  and  $\rho$ ;
2. run `applications-plots.exe` on this sample;
3. run `applications-fits.exe` on the resulting rootfile and store the output in `applications-plots-and-paper` subdirectory;
4. execute `make` in `applications-plots-and-paper` subdirectory.

Further details on each of these steps, including more technical details on the output and input files, are given in the distribution tar-ball and in the `README` files located in `TauSpinner/examples/applications` directory and all of the sub-directories.

The numerical results of whole paper can also be reconstructed. Scripts for most of the necessary operations are prepared and documented elsewhere in the paper or in `README` files.

## 5.2. Input file formats

Essentially any HepMC [28] file (saved in `HepMC::IO_GenEvent` format) can be processed<sup>14</sup>. Files with events stored in different format can be either converted to HepMC or interfaced using methods described in TauSpinner documentation and used in the default example `tau-reweight-test.cxx`.

---

<sup>14</sup> Note, however, that it is user responsibility to verify that HepMC file contains events with correctly structured information for TauSpinner to find outgoing  $\tau$  leptons and their decay products.

Note that only the file `applications-plots-and-paper/input-file-info.txt` should be updated by the user with the information on the event sample processed. All other text files will be updated by the appropriate tools described in the previous section. The content of these text files is included in the output file of pdf format, as shown in Appendix A.1 (available in the preprint version of the paper).

### 5.3. Rounding error recovering algorithm

The  $\tau$  leptons stored in data files can be ultra-relativistic. This may cause problems for the part of algorithm recalculating matrix elements for  $\tau$  decays. For our example, there was no problem with errors from rounding numbers but, in general, such problems are expected.

The following correcting algorithm is prepared:

1. For each stable  $\tau$ -decay product, its energy is recalculated from the mass and momentum.
2. The four-momentum of the  $\tau$  is recalculated from the sum of four-momenta of its decay products.
3. The algorithm performs check if resulting operation does not introduce sizable modifications, incompatible with rounding error recovery. If it does, a warning message is printed. This may indicate other than rounding error, difficulty with the production file. For example, some decay products not stored (*e.g.* expected as non-observable soft photons).

The algorithm is located in file `applications/CorrectEvent.h`. An example of its use is provided in `applications/hepmc-tauola-redecay.cxx`. By default, this algorithm is turned off.

### 5.4. Package use cases

This package can be used to validate several `TauSpinner` options representing different applications of `TauSpinner`. Such tests include, but are not limited to:

- A. **Applying longitudinal spin effects:** adding spin effect to an unpolarized sample using weights  $WT$  calculated by `TauSpinner`. For this purpose, set `Ipol=0` in the configuration file.
- B. **Removing spin effects:** removing spin effects from the polarized sample using weights calculated by `TauSpinner`. This is the default option used for our figures. The weight  $1/WT$  instead of  $WT$  should be used.

Note, that regardless of whether `Ipol=0` or `1`, `TauSpinner` works in the same manner. The two options are distinguished at the level of the user program only (use  $1/WT$  instead of  $WT$  to reweight events), as shown in our demo.

- C. **Working on the input file with spin correlations but without polarization:** initialize `TauSpinner` with `Ipol=2`. In this case,  $WT$  will represent correction necessary for implementation of the full longitudinal spin effects. Analogously, if the sample features  $\tau$  polarization but polarization is missing, the dependence on the  $\tau$ -leptons directions, `TauSpinner` should be initialized with `Ipol=3` and the missing dependence can be corrected with calculated weight  $WT$ .
- D. **Replacing spin effects of  $Z/\gamma^*$  with the Higgs-like spin-0 state spin correlations:** This could be realized with weights  $(\frac{1}{wt_{\text{spin}}})$  to remove spin effects of  $Z/\gamma^*$  times  $wt_{\text{spin}}^{\Phi}$  to introduce spin effects of  $\Phi$  without modification of event kinematics. Due to large spread in the weights, this method introduces large statistical fluctuations. Alternatively, this can be realized by regenerating  $\tau$  decays with `Tauola++` configured for the  $\tau$  pair originating from the scalar state resonance.
- E. **Validation:** test is similar to test A, we apply spin effect to a sample without polarization. However, for this test we take the polarized sample and replace its  $\tau$  decays by new, non-polarized ones using `Tauola++`. This allows to test different `Ipol` options as mentioned in test (C). It requires different setup and use of two input files. The `TauSpinner` should be executed on this new sample. The result should be then compared with the ones from *polarized* sample. Tools required to perform these steps are described in Sec. 5.1.4.

The results of the tests B and D are presented in the Appendices of a preprint version of this paper. The details of test C are described in `README of applications/testipol` subdirectory. Tools, that can be adapted to perform tests A and E, have been provided as well (see Sec. 5.1.4).

We have successfully performed tests A–E on samples generated with `Pythia8 + Photos++ + Tauola++` (in some cases `Pythia8` alone). Satisfactory results, of similar quality as discussed in our paper, Secs. 4.3 and 4.5 were always found. Further details for all of the cases listed above are given in the distribution tar-ball.

## 6. Summary

The paper presents the use of `TauSpinner` libraries for testing effects resulting from spin correlations and polarization of  $\tau$  leptons in processes at

the LHC featuring  $W$ ,  $Z$  and  $H$  decays. New example programs were developed and incorporated into program distribution tar-ball. The purpose of these programs is to analyse spin effects using information on the kinematics of  $\tau$ -decay products of events stored in a file. Moreover, they provide a convenient tool for validating the **TauSpinner** algorithms. As an important use case, this set of programs provides a method to evaluate systematic error on spin effect implementation in the so-called *embedded*  $\tau$  samples, an experimental technique used for analyses at the LHC.

For the purpose of presenting methodology, a set of kinematical distributions was selected and the physics properties of these distributions were explained on some example plots. Event samples featuring  $\tau$ -lepton decays of  $W$  and  $Z$  production at the LHC energies were generated. The weights calculated by **TauSpinner** algorithms were subsequently used to remove the effects due to polarization of decaying  $\tau$ . For comparison, the sample featuring no spin effects was also created on the flight. For studying the spin effects of the spin-0 intermediate state  $\Phi$ , the  $Z \rightarrow \tau\tau$  sample was modified, namely the  $\tau$ -leptons decay products were removed and the decays were generated again, using spin density matrix of  $H \rightarrow \tau^+\tau^-$  decay.

The details of the program installation and use were given. Our example provides test that algorithms of **TauSpinner** used for calculating spin weights are equivalent to the ones in **Tauola++**, the  $\tau$ -decay library used for creation of initial samples. We have also demonstrated how *physics history entries* of event samples can be used to provide validation tests for algorithm of effective Born level kinematic reconstruction and cross section calculations used in **TauSpinner**<sup>15</sup>.

The easiest cases to understand are the spin effects of  $\tau^\pm \rightarrow \pi^\pm \nu_\tau$  decays. The spectra are affected by spin as discussed in Ref. [10, 14], that is why we have frequently used this decay channel for the example plots of the paper. Due to  $Z$  polarization, there is clearly identifiable slope for the  $\pi^\pm$ s energy spectrum. The spin correlations of the two  $\tau$ s disfavour configurations when one of the  $\pi$  is hard and the other one is soft. For the  $\Phi \rightarrow \tau\tau$  case, the spin correlations effect is opposite.

For other  $\tau$  decay channels, effects of spin are more complex and we have presented results in the main body of the paper only for the  $\tau$ s of polarization originating from  $Z \rightarrow \tau\tau$  decays. Pattern of spin correlations and single  $\tau$ -polarization effect depends on the  $\tau$ -decay channel. One can easily notice

---

<sup>15</sup> In our paper, this method was used for comparisons with **Pythia8** results, which are of the leading logarithm precision level similarly as **TauSpinner**. Further extensions of this method is possible. Properties of factorization of exact QCD multiparton amplitudes need then to be used in the *physics history entries* of events stored by the reference generators. As one can see [21], such properties are present for QCD amplitudes, as it was the case of multiphoton amplitudes of QED which were used for  $\tau$ -lepton spin effects in KKMC Monte Carlo [29] of LEP applications.

from the lego plots that it will be affected by the kinematical selection on the other  $\tau$ -decay products as well, biasing the observed  $\tau$  polarization.

One should keep in mind when performing above tests that features of presented distributions depend strongly on the analysed event sample. If  $\tau$  leptons predominantly originate from the decays of  $Z$ ,  $W$ , or  $H$ , of virtualities close to the resonance peaks, and with the spin effects taken into account, the distributions should be similar to the ones presented in this paper. However, it might not always be the case. For results presented in this paper, parameters of the electroweak interactions and the PDFs used were carefully tuned between events generation and TauSpinner analysis codes. If this is not the case, particular patterns of discrepancies may appear. We will investigate this point in the future.

To evaluate sensitivity to the spin the average  $\tau$ -lepton polarization fits to the histograms of the simple analytic distributions are provided. The effects of QED bremsstrahlung or mass corrections are not incorporated into the functions used for fits in case of leptonic  $\tau$  decay. At LEP [11], it was shown that they may be of the similar size and shapes as polarization effects. We have also discussed that the alternative to analytical formulae, Monte Carlo based template distributions are useful for fits and evaluation of spin effects.

From the discussion presented in this paper, we left out discussion on functionality of matrix-element re-weighting described in Ref. [9]. This approach may be used to evaluate if spin effects present in a given sample can be helpful to distinguish different production mechanisms, ones combined with the effects of production distributions. In our present study, we however concentrated on discussing spin effects only.

We thank Prof. Erez Etzion for inspiring comment that bremsstrahlung effects given in semi analytical form (as in the LEP time CALASY program) may be of interest for the LHC applications as well. We thank Dr. Ian Nugent for careful and critical reading of our manuscript and for discussions. We thank Dr. Will Davey for discussions as well.

## REFERENCES

- [1] ATLAS Collaboration, [arXiv:0901.0512 \[hep-ex\]](#).
- [2] CMS Collaboration, [JINST 3, S08004 \(2008\)](#).
- [3] LHCb Collaboration, [JINST 3, S08005 \(2008\)](#).
- [4] ATLAS Collaboration, [Eur. Phys. J. C72, 2062 \(2012\)](#) [[arXiv:1204.6720 \[hep-ex\]](#)].
- [5] I. Deigaard, CERN-THESIS-2012-091.

- [6] J.L. Harton, *Nucl. Phys. Proc. Suppl.* **40**, 463 (1995).
- [7] A. Heister *et al.* [ALEPH Collaboration], *Eur. Phys. J.* **C20**, 401 (2001) [arXiv:hep-ex/0104038].
- [8] Z. Czyżczula, T. Przedziński, Z. Wąs, *Eur. Phys. J.* **C72**, 1988 (2012) [arXiv:1201.0117 [hep-ph]].
- [9] S. Banerjee *et al.*, *Eur. Phys. J.* **C73**, 2313 (2013) [arXiv:1212.2873 [hep-ph]].
- [10] S. Jadach, Z. Wąs, *Acta Phys. Pol. B* **15**, 1151 (1984); [Erratum *ibid.* **B16**, 483 (1985)].
- [11] P. Eberhard *et al.*, CERN-EP-89-129, C89-02-20.1, C89-05-08.2.
- [12] N. Davidson *et al.*, *Comput. Phys. Commun.* **183**, 821 (2012) [arXiv:1002.0543 [hep-ph]].
- [13] ATLAS Collaboration, ATLAS-CONF-2012-160.
- [14] T. Pierzchała, E. Richter-Wąs, Z. Wąs, M. Worek, *Acta Phys. Pol. B* **32**, 1277 (2001) [arXiv:hep-ph/0101311].
- [15] S. Jadach, Z. Wąs, R. Decker, J.H. Kühn, *Comput. Phys. Commun.* **76**, 361 (1993).
- [16] T. Sjöstrand, S. Mrenna, P. Skands, *Comput. Phys. Commun.* **178**, 852 (2008) [arXiv:0710.3820 [hep-ph]].
- [17] N. Davidson, T. Przedziński, Z. Wąs, arXiv:1011.0937 [hep-ph].
- [18] G. Altarelli, R. Kleiss, C. Verzegnassi, CERN-89-08-V-1.
- [19] G. Altarelli, R. Kleiss, C. Verzegnassi, CERN-89-08-V-3.
- [20] W. Verkerke, D. Kirkby, arXiv:physics/0306116v1 [physics.data-an].
- [21] A. van Hameren, Z. Wąs, *Eur. Phys. J.* **C61**, 33 (2009) [arXiv:0802.2182 [hep-ph]].
- [22] E. Mirkes, *Nucl. Phys.* **B387**, 3 (1992).
- [23] E. Mirkes, J. Ohnemus, *Phys. Rev.* **D50**, 5692 (1994) [arXiv:hep-ph/9406381].
- [24] T. Aaltonen *et al.* [CDF Collaboration], *Phys. Rev.* **D88**, 072002 (2013) [arXiv:1307.0770 [hep-ex]].
- [25] R. Kleiss, *Nucl. Phys.* **B347**, 67 (1990).
- [26] Z. Wąs, S. Jadach, *Phys. Rev.* **D41**, 1425 (1990).
- [27] N. Davidson *et al.*, Tauola and Tauola C++ Interface source code and documentation available from <http://wasm.web.cern.ch/wasm/C++.html> or <http://tauolapp.web.cern.ch>
- [28] M. Dobbs, J.B. Hansen, *Comput. Phys. Commun.* **134**, 41 (2001) [<https://savannah.cern.ch/projects/hepmc/>].
- [29] S. Jadach, B. Ward, Z. Wąs, *Comput. Phys. Commun.* **130**, 260 (2000) [arXiv:hep-ph/9912214].